TECHNICAL RESEARCH REPORT

SYSTEMS RESEARCH CENTER

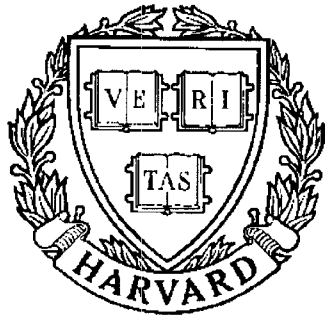

Supported by the National Science Foundation Engineering Research Center Program (NSFD CD 8803012), the University of Maryland, Harvard University, and Industry

Predicting the Complexity of Disconnected Basins of Attraction for a Noninvertible System

by R.A. Adomaitis, I.G. Kevrekidis and R. de la Llave

TR 91-41

Predicting the Complexity of Disconnected Basins of Attraction for a Noninvertible System

Raymond A. Adomaitis, Systems Research Center, University of Maryland
Ioannis G. Kevrekidis, Department of Chemical Engineering, Princeton University
Rafael de la Llave, Department of Mathematics, University of Texas

Manuscript date: April 1991

Abstract

A noninvertible, two-dimensional, discrete-time system featuring multistability is presented. Because the preimage behavior of this system is a function of location in phase space, the boundary separating the basins of attraction can be disconnected. These "polka-dot" basins of attraction have either a finite number of preimages (giving a finitely-complicated basin) or infinitely many (giving infinite complexity). A complexity criterion based on following the noninvertible region forward in time is presented and a fixed-point algorithm for computing the boundary of the "complete" noninvertible region is discussed.

Introduction

A nonlinear system having multiple, stable, equilibrium states will have a phase space divided by the boundaries of the different basins of attraction. In an invertible system, these boundaries are invariant objects defined by the points in phase space which, when followed forward in time, do not asymptotically approach any of the attractors. These objects are typically the stable manifolds of fixed or periodic saddle-type points or of invariant circles. The manifolds themselves can undergo global bifurcations or transitions giving complicated, but reasonable-well understood behavior. It is important to note that while the basins of attraction may have complicated, contorted boundaries, the basins themselves remain as contiguous regions of phase space.

Maps that are noninvertible allow distinctly-different points in phase space to be mapped to a single point in one forward iteration of the map. Furthermore, the number of the points which are mapped to one (i.e., the preimage behavior) can change as a function of the location in phase space. This underlying structure profoundly affects the geometry of the basin boundaries (in particular, can give rise to discontinuous, polka-dot-like basins of attraction) and also influences the shape and location of the attractors (Gumowski and Mira, 1980). In this note, we show that following selected patches of phase space forward in time gives insight and computable conditions for determining the point in parameter space separating polka-dot basins of finite and infinite complexity and determining which portions of phase space an attractor cannot inhabit—recall that equilibrium states cannot be found in noninvertible regions.

The system analyzed is the Rotating Logistic map:

$$(r,\theta) \mapsto F(r,\theta) \quad \text{where} \quad F(r,\theta) = (r^2 + \lambda + \epsilon \cos 2\pi\theta, \theta + \omega \mod 1) \tag{1}$$

with ω irrational (Kevrekidis *et al.*, 1985; Adomaitis, 1990). Because of the constant rate of rotation and the choice of $\omega = (\sqrt{5}-1)/2$, the system will never exhibit fixed or periodic points and will only have equilibrium states in the form of invariant circles and other, more complicated objects. Also, one can prove that in the limit of $\epsilon \to 0$, the invariant circles will be smooth and will demonstrate the same bifurcation behavior as the logistic map: a saddle-node bifurcation of invariant circles at $\lambda = 1/4$ and a supercritical cascade (in the direction of decreasing λ) of period-doubling bifurcations beginning with the period-doubling of the period-1 invariant circle at $\lambda = -3/4$.

The only attractors of this system are the bounded invariant object born during the saddle-node bifurcation and the attractor at $r \to \infty$ (see Fig. 1 for a representative situation). At first glance, it appears that the boundaries separating the basins of attraction would be provided by the unstable invariant circle and its negative preimage. As seen in Fig. 2a, this is true under some circumstances, but as seen in Fig. 2b, this is not always true. The latter Figure demonstrates that the basin of attraction of the attractor at infinity can extend into the "apparent" basin of attraction of the bounded attractor in the form of "polka-dots" of phase space. The mechanism that gives rise to polka-dots is illustrated in Fig. 3a: when the boundary separating the region where two real preimages exist (the upper, 2RP region) from the zero-real-preimage region (the 0RP region) of the period-1 map (1) has a segment which exists below the negative-root preimage line, polka-dots exist and can be computed by following the preimages of this first polka-dot (Adomaitis, 1990; Gumowski and Mira, 1980). The first polka-dot acts as a window which allows a region of the apparent basin of attraction (the region of phase space in between the unstable invariant circle and its negative-root preimage) to be mapped above the unstable invariant

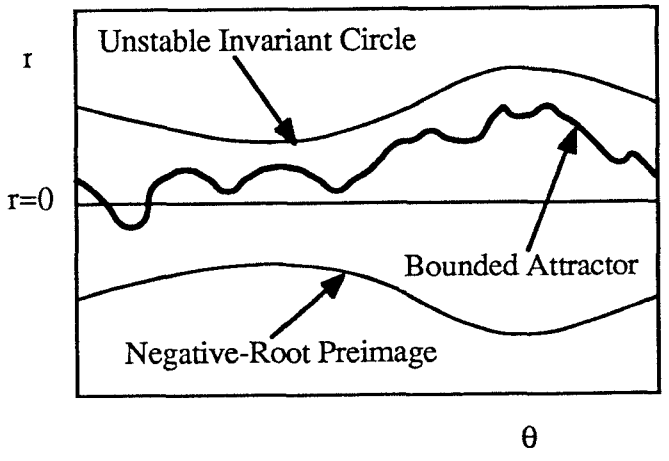

Fig. 1. A representative phase portrait of the Rotating Logistic map.

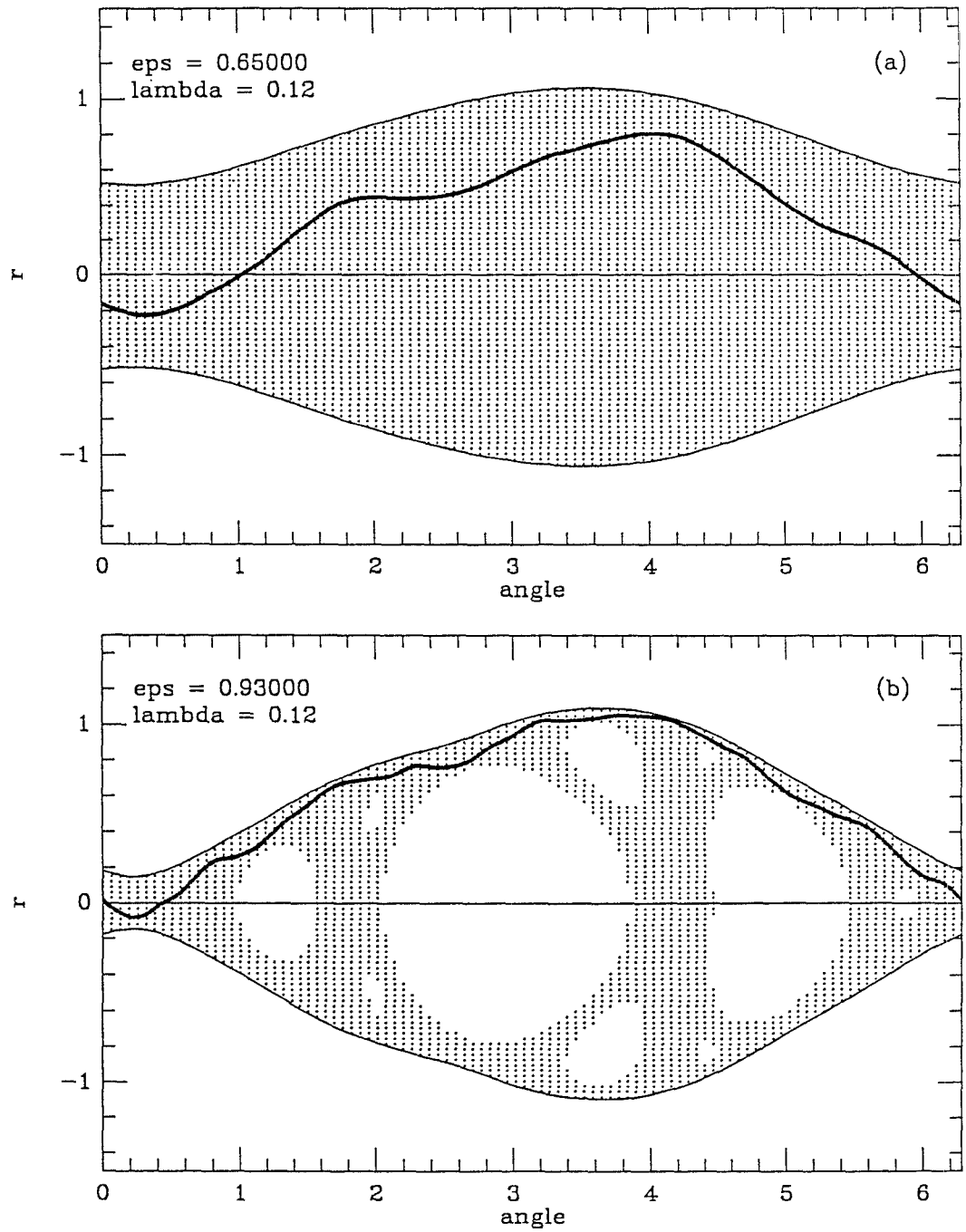

Fig. 2. Results from "brute-force" calculations of the basin of attraction of the bounded solution illustrating (a) an "expected" basin structure and (b) polka-dots in the expected basin. The white regions are the basin of attraction of the $r \to \infty$ attractor.

circle (and subsequently towards positive infinity) in one forward iteration. A key notion needed to understand the polka-dot behavior is how the phase space folds in one forward iteration (see Fig. 3b)—since both the upper and lower boundaries of the apparent region map to the unstable invariant circle, the phase space must fold along some curve. This curve is defined by setting the determinant of the Jacobian matrix equal to zero: in (1) it is simply $r = 0$ (the one-dimensional return map of Fig. 3b can be thought of as a "cut" of F parameterized by θ). Thus, the unstable invariant circle and the image of $r = 0$ provide the boundaries of the *image* of the apparent region. As was also shown in Yasuda and Sunahara (1990), if this image lies within the original region no polka-dots are to be expected, and if some part of the image falls outside polka-dots are to be expected and can be computed by following all of the preimages of this region.

Comparing Figs. 4a and 4b brings to light another issue: under some circumstances (Fig. 4a) we see that all of the polka-dot preimages eventually premap into the 0RP region giving finite complexity to the basin of attraction, and for a different set of parameter values the polka-dots can be premapped *ad infinitum* (Fig. 4b) giving infinite complexity. The case of a finite number of polka-dot preimages is equivalent to following the 0RP region (the boundary is defined by inverting (1) and determining where the inverse has a single, real root: $r = \epsilon \cos 2\pi(\theta - \omega) + \lambda$) *forward* in time, accumulating the regions of phase space defined by the overlapping region of the folded image of the regions accumulated. Iterating this algorithm determines the "complete" noninvertible region: the union of the 0RP region and the region of phase space in which *all* of the preimages eventually premap to the 0RP region. We see that if the "first" polka-dot is contained *within* the complete noninvertible region, there will be a finite number of preimages of the first polka-dot. If any portion of the first polka-dot lies outside the complete region, that portion will have an infinite number of preimages. It should also be noted that equilibrium states must lie outside the complete region since any point on a equilibrium solution has an infinite number of preimages.

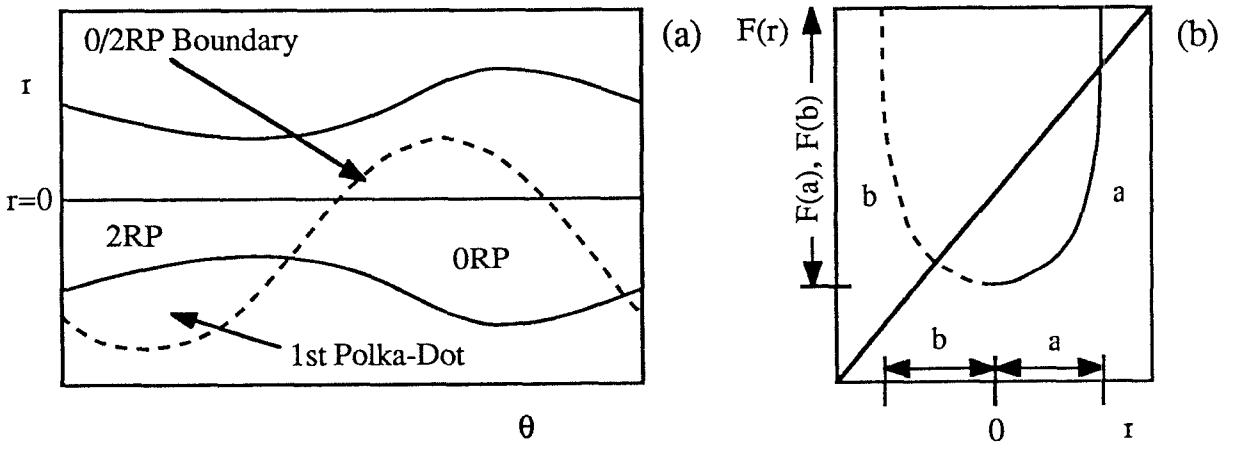

Fig. 3. (a) The varying preimage behavior and (b) an illustration the folding behavior of a one-dimensional, noninvertible system.

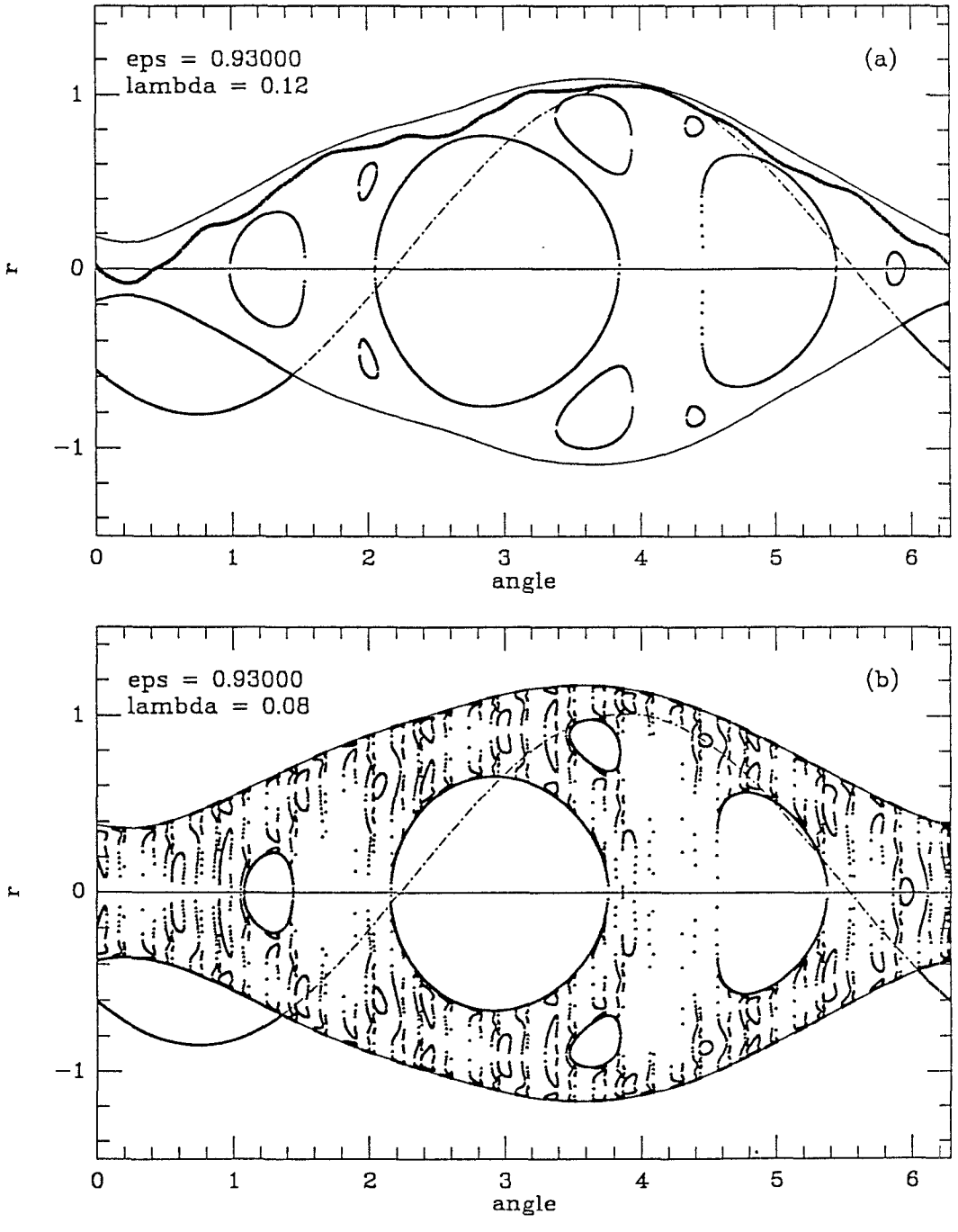

Fig. 4. Results of preiterating the first polka-dot: (a) A finitely-complicated basin structure; (b) Infinite complexity.

It now appears that we have only replaced following polka-dots backward in time with following folding fragments of phase space forward in time, possibly without end, as a means of determining the complexity of the polka-dot structure. However, it will be shown in the next section that for the Rotating Logistic map (and possibly other maps):

1) The portions of the images of the union of the 0RP region and the regions which eventually premap to the 0RP region "glue" onto the 0RP region giving a larger, closed (in the sense that it has no holes) region;

2) The edges of the images glue smoothly onto the 0RP region giving the complete noninvertible region smooth boundaries;

3) The intersection of the folded image of the union of the 0RP region and the regions which eventually premap to the 0RP region are simply the image of the "accumulated" region above $r = 0$;

4) The positive segment of the boundary of the complete noninvertible region maps onto a portion of itself and the remainder onto the negative segment—the boundary is thus invariant under the map in a limited way. This means that while it is not an equilibrium state of (1), we can write a fixed-point algorithm for computing it, hence, the infinite-complexity condition can be computed in a finite amount of time (an amount roughly on the order of computing the onset-of-polka-dots condition).

Folding Under Forward Iteration

Consider the situation illustrated in Fig. 5, where the unstable invariant circle, it negative-root preimage, and the boundary separating the 0RP from the 2RP regions are shown. We see that a sizable portion of the 0RP region stretches into the apparent basin of attraction of the bounded attractor. This region is divided into two, the upper marked A and the lower B, by the $\det(\mathbf{J}) = 0$ condition ($r = 0$). Returning to the one-dimensional parameterization of F illustrated in Fig. 3b, it becomes easier to visualize how the phase space folds along $r = 0$; the image of A retains its orientation and the image of B is flipped. Both images are connected at $F(r = 0)$ and so we have a region $F(A) \cap F(B)$ which is, in effect, a noninvertible region since both preimages of this region come from the 0RP region in one forward iteration. Another important fact becomes apparent when $F(A)$ and $F(B)$ are plotted (Figs. 5a and 5b): because the boundary separating the 0RP and 2RP regions is the image of the folding line ($r = 0$), the regions which eventually premap into the 0RP region are *always* "glued" to the 0RP region, making the "accumulated" noninvertible region a connected, hole-less region.

If we inspect the images of the two regions where the boundary separating the 0RP and 2RP regions intersects $r = 0$, we see that since F preserves smoothness, since $r = 0$

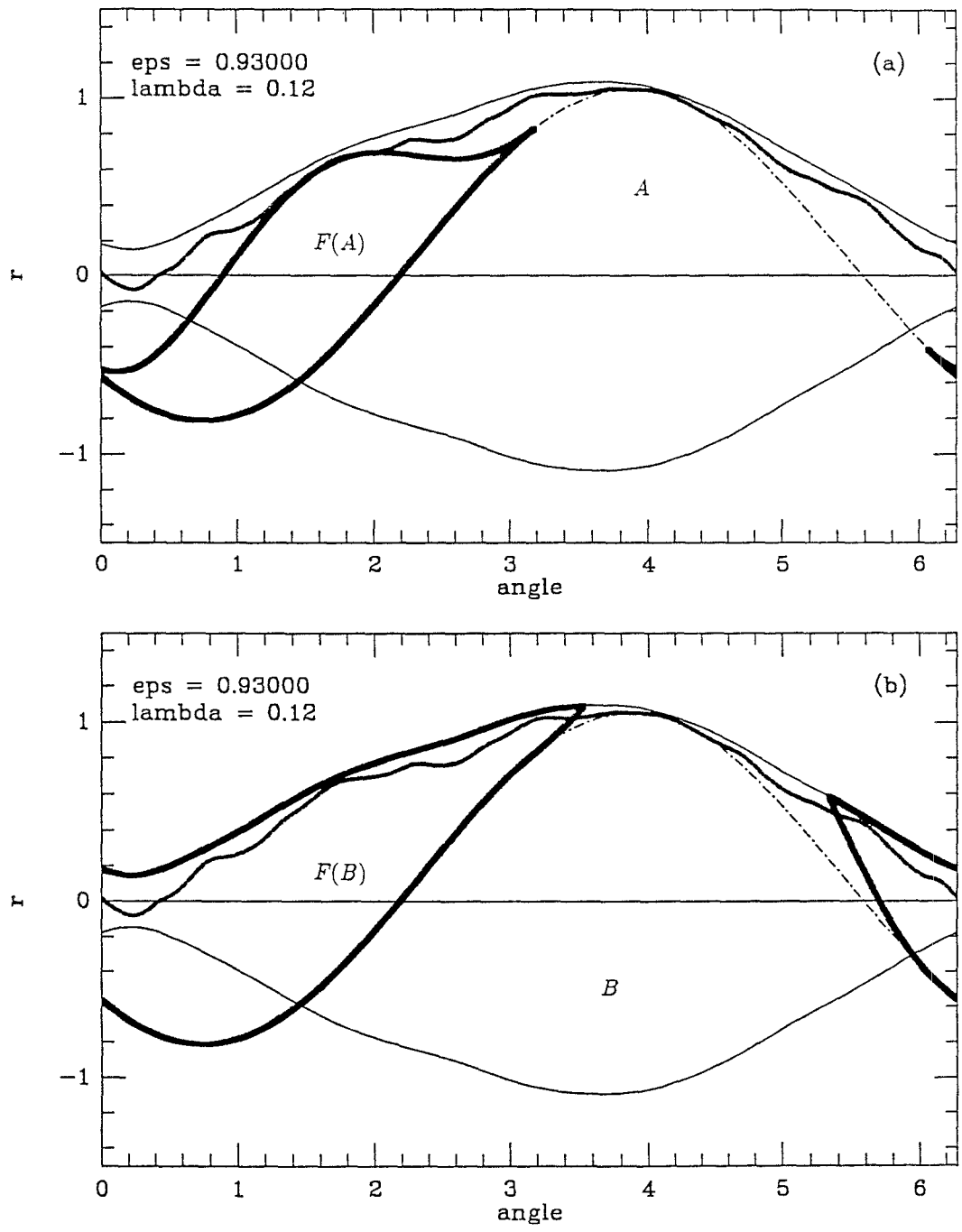

Fig. 5. Images of the 0RP region above the negative-root preimage line: (a) The positive portion A; (b) The negative portion B.

maps to the 0RP/2RP boundary, and since nothing can be mapped into the 0RP region, the images of the 0RP/2RP boundary must bend towards, touch the 0RP/2RP boundary tangentially, and then bend back. This means that the portions glued to the 0RP region glue *smoothly* and will give a complete noninvertible region that is smooth.

The following facts (especially fact (3) of the previous section) appear to be specific to F, although some of the ideas should be applicable to other maps. This third issue concerns computing the intersection of the folded image of the "accumulated" region (the 0RP region plus n image intersections where n is less than that required to find the complete region). First, there are two things to note:

a) The negative-root preimage of the unstable invariant circle can never cross $r = 0$ (proof is obvious);

b) No point in the region below the unstable invariant circle and above $r = 0$ can be mapped in a single iteration to a point above the unstable invariant circle (proof is based on the unstable invariant circle mapping to itself and $r = 0$ being the $\det(\mathbf{J}) = 0$ condition—the image of this region has the same orientation so the images of the two boundaries cannot intersect).

With these two facts in mind and looking at Fig. 5, we see that area B extends (with respect to θ) beyond region A. By (b) we know that A will always remain below the unstable invariant circle but B will be flipped with its bottom mapped to the unstable invariant circle and its top mapped to the same segment as the bottom of A. Because the rate of rotation (with respect to θ) is independent of r and because B extends beyond A, we see that $F(A) \cap F(B) = F(A)$ whenever the accumulated noninvertible region has this lemon-shape with $r = 0$ passing through the upper part of the "lemon" (and by (a), it always will).

After this first iteration, we see that the accumulated region consists of $F(A) \cup 0\text{RP}$ and anything premapped into this region will either have zero preimages or will have one or two real preimages inside the 0RP region. Because of the way $F(A)$ glues onto the 0RP region, the basic shape of the accumulated region remains unchanged and so the intersection of the two folds of the accumulated region always consists of the image of the positive portion. We can also see at this time that since the orientation of the image of the positive portion is preserved and since the lower boundary of the positive portion is mapped onto the 0RP/2RP boundary, the upper boundary of the accumulated region can be computed by iterating on the map:

$$G(r,\theta) = \begin{cases} (r^2 + \lambda + \epsilon\cos 2\pi\theta, \theta + \omega) & \text{for } r > 0; \\ (\lambda + \epsilon\cos 2\pi\theta, \theta + \omega) & r \le 0, \end{cases} \tag{2}$$

with the initial condition

$$\Gamma_{\text{pos},0}(r,\theta) = \begin{cases} r = \epsilon\cos 2\pi(\theta - \omega) + \lambda & \text{for } \epsilon\cos 2\pi(\theta - \omega) + \lambda > 0; \\ r = 0 & \epsilon\cos 2\pi(\theta - \omega) + \lambda \le 0. \end{cases} \tag{3}$$

The complete noninvertibility region boundary is a stable equilibrium solution to G. It is interesting to note that when the complete noninvertibility region boundary lies completely above $r = 0$, the stable attractor and the complete noninvertibility boundary coincide.

The Fixed-Point Algorithm

In the previous section, it was shown that the upper boundary of the accumulated noninvertible region could be found iteratively with the iterations converging to the upper boundary of the complete noninvertible region. Just as with any other equilibrium solution, this procedure can be sped up using a Newton-Raphson algorithm. Since it has been shown that the upper boundary of the complete noninvertible region is smooth and otherwise well-behaved, it seems reasonable that a discretization of the entire upper boundary $\Gamma(\theta)$ should capture the correct behavior. Thus, the irrational ω will be approximated by the ratio of two consecutive terms in the Fibonacci sequence $\omega = f_{n-1}/f_n$ and so the Newton algorithm can be written as

$$\Gamma_0^2(\theta_i) + \lambda + \epsilon\cos 2\pi\theta_i - \Gamma_0(\theta_i) = [\Gamma_1(\theta_j) - \Gamma_0(\theta_j)] - 2\Gamma_0(\theta_i)\,[\Gamma_1(\theta_i) - \Gamma_0(\theta_i)] \qquad (4a)$$

for $\Gamma_0(\theta_i) > 0$ and

$$\lambda + \epsilon\cos 2\pi\theta_i - \Gamma_0(\theta_i) = [\Gamma_1(\theta_j) - \Gamma_0(\theta_j)] \quad \text{for} \quad \Gamma_0(\theta_i) \le 0. \qquad (4b)$$

In the above, $\theta_i = i/f_n$, $\theta_j = (i + f_{n-1})/f_n \bmod f_n + 1$, and the subscript 0 denotes the results of the previous Newton iteration and 1 the present. An example of the results of this algorithm can be seen in Fig. 6. The quantity d is the minimum vertical distance from the complete noninvertibility region boundary to the first polka-dot. A positive d therefore indicates finite complexity and negative indicates infinite complexity.

Two-Parameter Continuations

As mentioned previously, the bifurcation behavior of the invariant circles is equivalent to the logistic map in the limit of $\epsilon \to 0$. However, as ϵ is increased the behavior changes and it becomes more difficult to draw analogies with the logistic map. A partial classification of qualitatively-different behaviors is given in Fig. 7.

For large λ all forward iterations approach positive infinity. For small ϵ, decreasing λ means eventually passing through a saddle-node bifurcation of invariant circles, giving rise to a stable and unstable invariant circle which exist in the region marked "2 ICs" in Fig. 7. Keeping $\lambda = 0.1$ and increasing ϵ from $\epsilon \to 0$, we see that the stable invariant circle eventually touches the noninvertibility curve (the image of $r = 0$). No transition takes place at this point, but this curve is connected to the onset-of-polka-dots curve (the latter is shown as the dotted curve of Fig. 7). Also, notice that while touching the noninvertibility

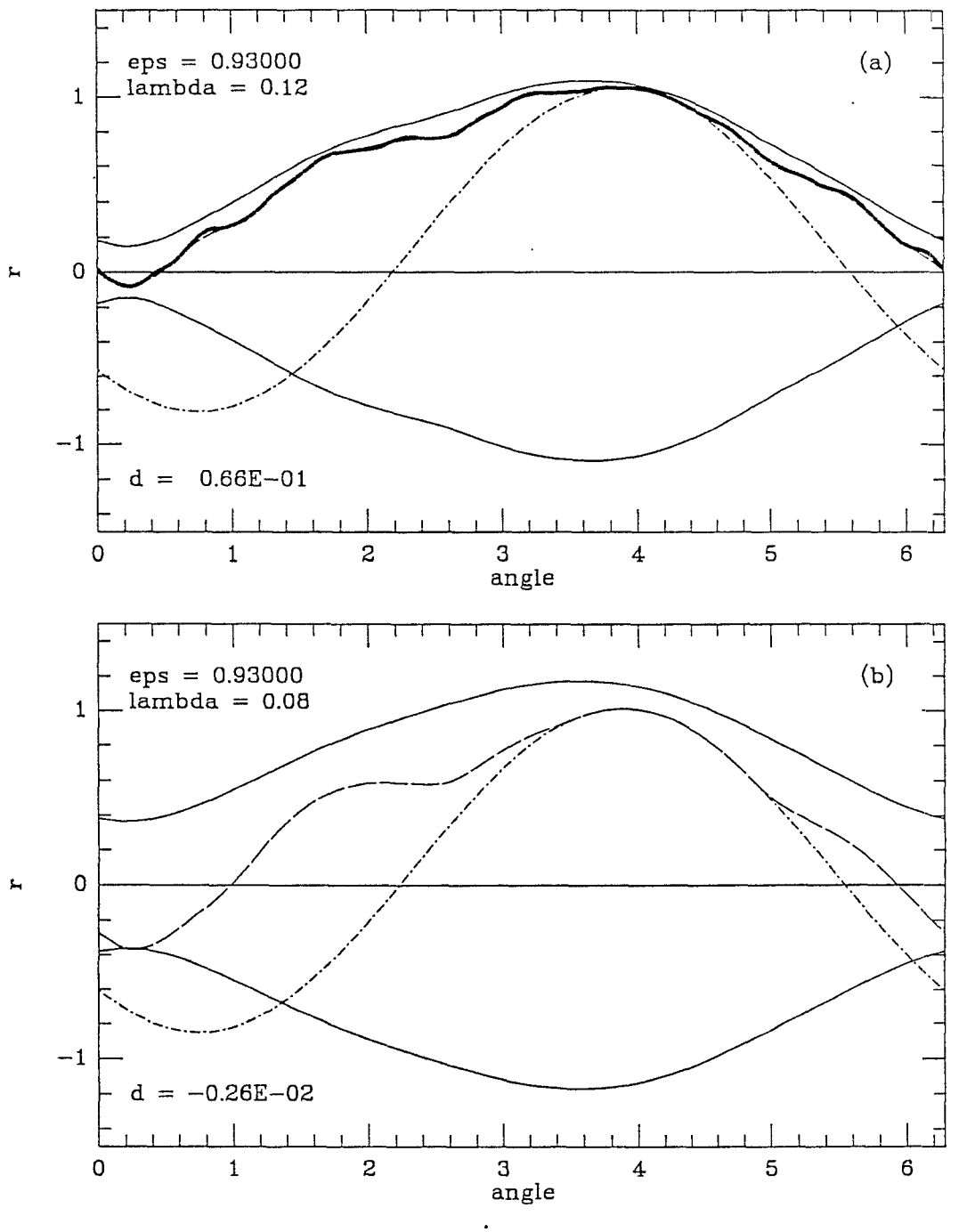

Fig. 6. The complete noninvertible region upper boundary computed by the fixed-point algorithm (shown as the long-dashed line): (a) Finite complexity case (note how the bounded attractor nearly coincides with the boundary); (b) Infinite complexity case. No attractor was found in this case. (Infinite complexity = destruction of the attractor? Maybe, maybe not.)

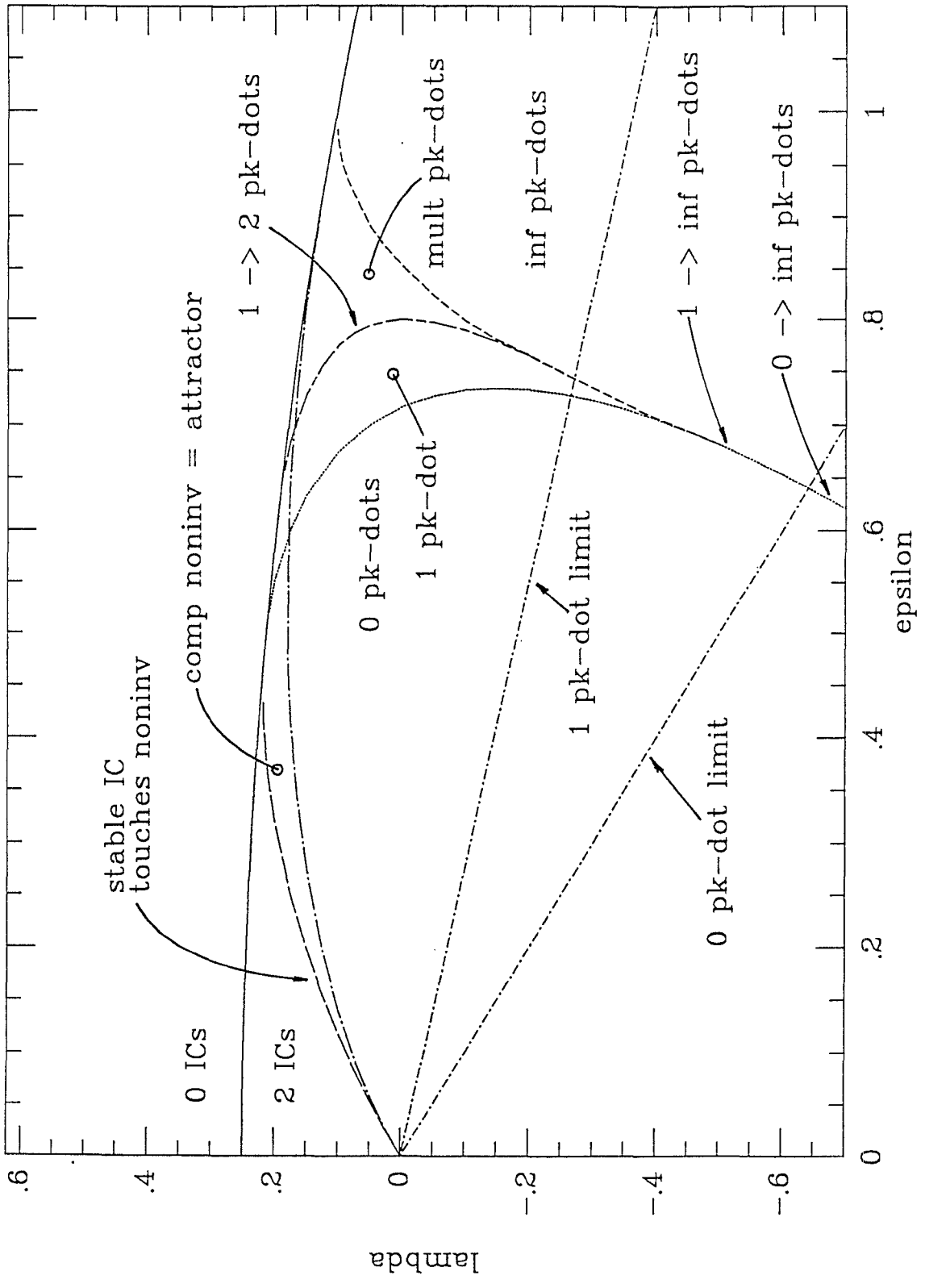

Fig. 7. A partial classification of the qualitatively-different dynamical behaviors exhibited by the rotating logistic map in two of its parameters.

curve is a *necessary* consequence of the attractor crossing $r = 0$, the reverse is not always true, so the attractor remains as the boundary of the complete noninvertible region of phase space until the long-dash-dot curve is crossed.

We are now in the region where the attractor lies both above and below $r = 0$ and still have an "apparent" basin of the bounded attractor unpopulated by polka-dots. Continuing to increase ϵ, we cross the onset-of-polka-dots line. For λ above the the curve marked "1 pk-dot limit", only one polka-dot is found in the apparent basin of attraction. Proof of this can be seen with a single iteration of the positive portion of the "lemon" for λ below this curve—it is completely mapped into $r < 0$ in a single iteration. Furthermore, by plotting the curve of where the top of the noninvertible region touches $r = 0$ (given by $\lambda = \epsilon$), we see that below this curve, the noninvertible region *is* the complete noninvertible region, hence, the onset of polka-dots corresponds to the onset of infinite complexity.

We have computed other curves, such as the transition from one polka-dot to two, and so-forth. The final question is whether the onset of infinitely many polka-dots implies the destruction of the attractor. Careful computations for $\lambda = -0.7$ indicate this might be the case, at least for this particular parameter value.

Conclusions

A noninvertible, two-dimensional map featuring a complicated, disconnected basin of attraction structure was discussed. A fixed-point algorithm for computing the boundary of the "complete" noninvertible region (the region of phase space that has no preimages plus the portion of phase space which gets completely premapped into it) was developed and was used to predict the complexity level of the basin structure.

Acknowledgment

RAA acknowledges the support of the SRC through NSF grant ECD-8803012-06.

References

Adomaitis, R. A. (1990). The Rotating Logistic Map: Polka-Dots in the Basin of Attraction. *Personal Correspondence to R. de la Llave and I. G. Kevrekidis*

Gumowski, I. and C. Mira (1980). *Recurrences and Discrete Dynamic Systems*,Lecture Notes in Mathematics #809, Springer-Verlag, Berlin.

Kevrekidis, I. G., R. Aris, L. D. Schmidt, and S. Pelikan (1985). Numerical Computation of Invariant Circles of Maps. *Physica D*, **16**, 243-251.

Yasuda, T. and Y. Sunahara (1990). Stabilization of a Chaotic Preditor-Prey System Considering Fractal Boundaries. *Proc. 11th IFAC World Congress, Tallinn*, **6**, 129-134.